Pure Appl. Chem., Vol. 81, No. 6, pp. 1123–1129, 2009.
doi:10.1351/PAC-CON-08-08-37

Ion channel complex of antibiotics as viewed by NMR*

Michio Murata‡, Yusuke Kasai, Yuichi Umegawa, Naohiro Matsushita, Hiroshi Tsuchikawa, Nobuaki Matsumori, and Tohru Oishi

Department of Chemistry, Graduate School of Science, Osaka University, 1-1 Machikaneyama, Toyonaka, Osaka 562-0043, Japan

Abstract: Amphotericin B (AmB) exerts its pharmacological effects by forming a barrel-stave assembly in fungal membranes. To examine the interaction between AmB and ergosterol or cholesterol, ^{13}C- and ^{19}F-labeled covalent conjugates were prepared and subjected to solid-state NMR measurements. Using rotor-synchronous double-resonance experiments such as rotational echo double resonance (REDOR) and RDX, we estimated the distance between the fluorine atom and its nearest carbon in the heptaene moiety to be less than 8.6 Å, indicating that the B ring of ergosterol comes close to the AmB polyene moiety. Conformational search of the AmB–ergosterol conjugate using the NMR-derived constraints suggested that ergosterol molecules surround the AmB assembly in contrast to the conventional image where ergosterol is inserted into AmB molecules. AmB–AmB bimolecular interaction was examined by using ^{13}C- and ^{19}F-labeled AmBs in dimyritoylphosphatidylcholine (DMPC) membrane without sterols. ^{13}C-^{19}F dipolar interactions deriving from both head-to-head and head-to-tail orientations were observed in the REDOR experiments. The interactions between AmB and acyl chains of the phospholipid were also detected.

Keywords: amphotericin B; solid-state NMR; ergosterol; cholesterol; lipid bilayer.

INTRODUCTION

The mechanism of action of antibiotics attracts growing attention in the pharmaceutical sciences [1]. Because the appearance of antibiotic-resistant microbes poses a serious threat to publish health, antibiotics with protein targets tend to have a shorter market value. On the other hand, amphotericin B (AmB, **1**) has been used as an antifungal drug for over 40 years and still possesses clinical importance largely due to its non-protein target [2,3]. The drug has a specific interaction with membrane sterols upon forming an ion channel assembly. The selective toxicity of AmB against fungi is generally accounted for by its higher affinity to ergosterol than cholesterol. When comparing them in dissociation constants, ergosterol has one-order higher affinity to AmB than dose cholesterol [4]. Thus, the toxicity against the yeast *Candida albicans*, whose membrane sterol is ergosterol, is 60 times more potent than hemolytic activity to human blood cells, which contain cholesterol [5]. Figure 1 shows a hypothetical picture of the AmB ion channel, called a "barrel-stave model", which comprises about eight pairs of AmB/sterol [6]. The hydrophobic polyene parts of AmB face outside to interact with fatty acid chains while hydrophilic polyhydroxyl groups face inside to form channel lining. Ergosterol is supposed to sta-

*Paper based on a presentation at the 26th International Symposium on Chemistry of Natural Products (ISCNP-26) and 6th International Conference on Biodiversity (ICOB-6), 13–18 July 2008, Charlottetown, Prince Edward Island, Canada. Other presentations are published in this issue, pp. 1001–1129.

‡Corresponding author

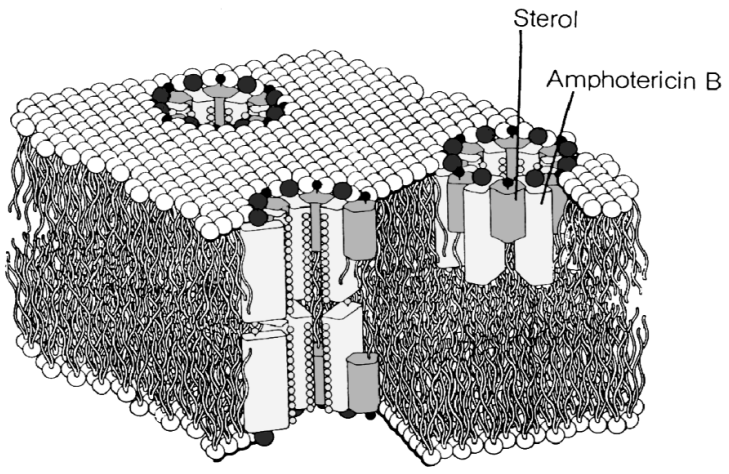

Fig. 1 Hypothetical "barrel-stave" model proposed by De Kruijff et al. [6].

bilize the channel complex by acting as glue to connect AmB molecules. However, no direct evidence for this model has been hitherto obtained.

Rotational echo double resonance (REDOR or RDX) is one of the solid-state NMR techniques to determine the distance between two labeled atoms [7]. In this pulse sequence (Fig. 2), when fluorine atoms are irradiated at an interval synchronous to the rate of magic angle spinning, specific dipole interaction is regenerated, which is otherwise eliminated by fast magic angle spinning. This regeneration of dipole coupling results in a decrease of ^{13}C NMR peaks located in the vicinity of the irradiated fluorine atom (dephasing effects). The peak reduction ratio is proportional to the inverse cubic of an interatomic distance. When the experimental data fits a theoretical curve, an interatomic distance can be determined with the accuracy of 0.1 Å. In the present study we report the AmB-sterol and AmB-AmB interactions as viewed by solid-state NMR, particularly using REDOR and RDX.

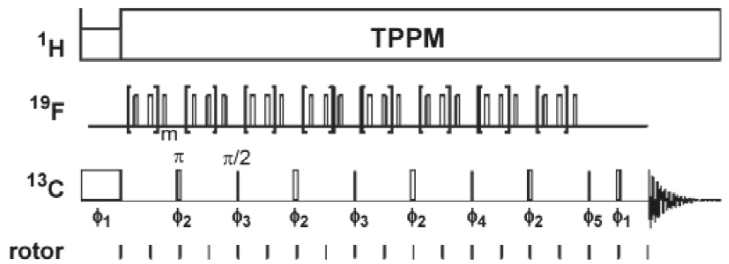

Fig. 2 Pulse sequence of $^{13}C\{^{19}F\}$ RDX. ^{13}C-^{13}C spin-spin coupling is suppressed by π/2 pulses for ^{13}C nuclei. TPPM, two-pulse phase modulation; ϕ, phase cycles for ^{13}C pulses [7c].

AmB–STEROL CONJUGATES

The mechanism of bimolecular recognitions between AmB and AmB or AmB and sterol is essential for elucidating the structure of this channel assembly [8–13]. Ergosterol is shown to interact with AmB, but their affinity turned out to be relatively weak for detecting intermolecular interactions in REDOR experiments. In order to stabilize the AmB–sterol interaction, we prepared labeled compounds and conjugated them covalently as depicted in Scheme 1 [12]. Uniformly labeled AmB was prepared by feed-

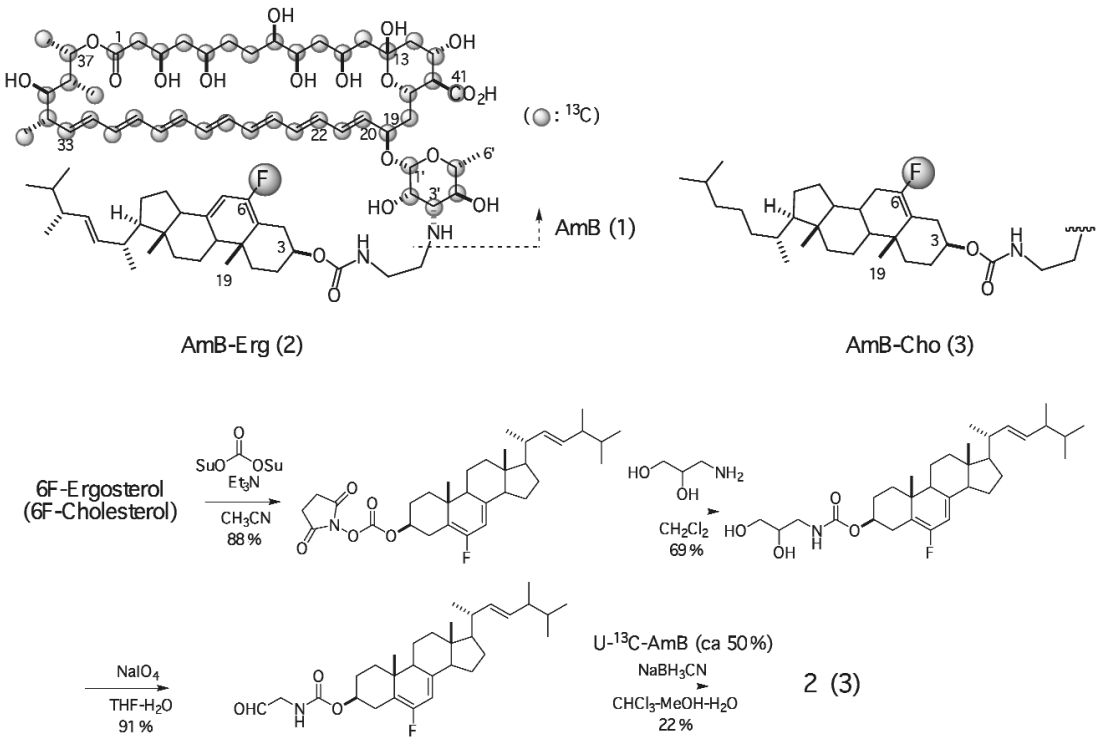

Scheme 1 Preparation of AmB–sterol conjugates **2** and **3** [12,16].

ing the drug-producing organism *Streptomyces nodosus* with $^{13}C_6$-labeled glucose. Since AmB is a polyketide metabolite, carbon atoms in aglycon are originated from acetate and propionate, which are further derivable from ^{13}C-enriched glucose. In the post polyketide synthesis steps, glucose is to be directly incorporated into the mycosamine residue, which furnishes uniformly ^{13}C-enriched AmB (average 50 % enrichment). For the chemical preparation of AmB–sterol conjugates (Scheme 1), fluorinated ergosterol [14] or cholesterol [15] was first converted to an activated carbonate ester. Then, amide formation furnished a carbamate intermediate. Periodate oxidation gave rise to an aldehyde, which was then subjected to reductive aminoalkylation with uniformly ^{13}C-labeled AmB. AmB–sterol conjugates (**2** and **3**) were obtained in the total yield of about 10 % [16]. Conjugates **2** and **3** were subjected to modified version of REDOR experiments (RDX) [7c]. The method was developed to measure REDOR with multiply ^{13}C-labeled compounds. As shown in Fig. 3, the dephasing effect of 12 % was observed for the polyene signals of AmB. We deduced the distance between the fluorine atom and its nearest carbon of the heptaene moiety in **2** to be less than 8.6 Å. The same RDX experiments, which were carried out in the presence of the same amount of non-labeled conjugate, revealed a similar reduction for the polyene peak. The result indicates that the RDX dephasing is caused by intramolecular interaction rather than intermolecular one. Cholesterol conjugate **3** showed dephasing effects to a similar extent, suggesting that the higher affinity to ergosterol can be easily compensated by covalent conjugation. Nonconjugated pair of ^{13}C-labeled AmB and 6-fluoroergosterol gave rise to no RDX dephasing in DMPC membrane. These data suggest the that AmB–ergosterol interaction is not so strong as deduced from the conventional barrel-stave model, where sterol is inserted between two AmB molecules (Fig. 4). Rather, it interacts with polyene from the outside. To precisely deduce this bimolecular interaction, a molecular modeling study was carried out using MacroModel under the following conditions; Macromodel ver. 8.6; molecular field, AMBER*; solvent, water (GB/SA model); energy minimization,

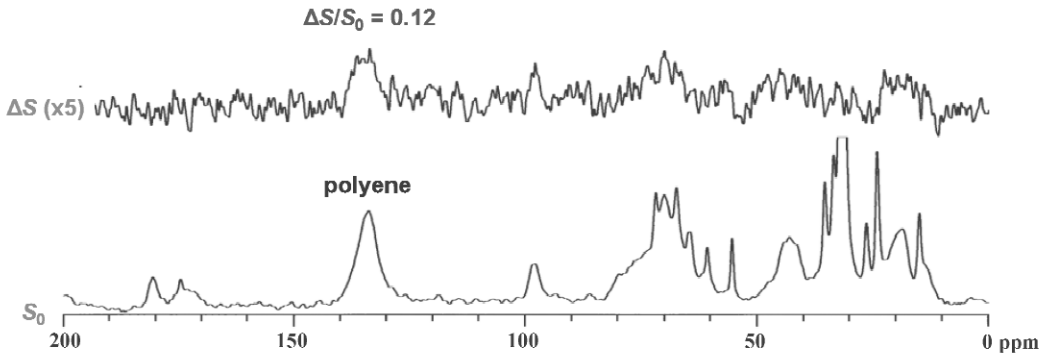

Fig. 3 $^{13}C\{^{19}F\}$ RDX spectra of AmB–ergosterol conjugate **2** in DMPC membrane [16].

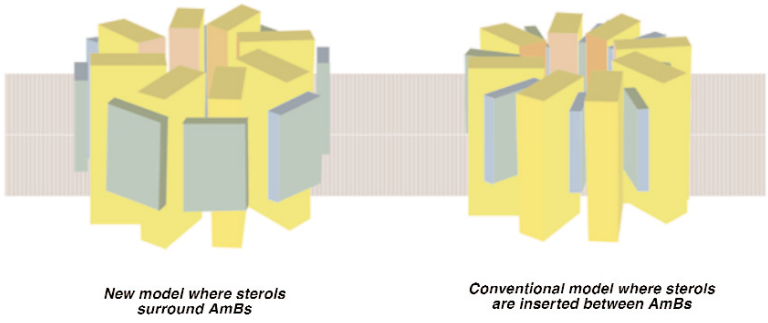

Fig. 4 New surrounding model (left) for AmB–ergosterol interaction in comparison with a conventional model (right) [16].

PRCG; conformation generate, CMM; and distance constraint, C(23)/6-F: (5.4 ± 3.0) Å. Nine bonds between AmB aglycone and ergosterol were allowed to rotate with the NMR-derived distance constraint during the calculations. One of the most stable conformers thus obtained revealed that the β-plane of ergosterol alicycle faced to the π-plane of heptaene rather than being sandwiched between macrolactone planes [16]. With these data in hand, we proposed a new model for AmB–ergosterol interaction as shown in Fig. 4.

AmB–AmB INTERACTIONS

In the next step, we examined the AmB–AmB interactions by solid-state NMR. Selectively labeled AmBs with ^{13}C and ^{19}F were prepared by chemical and biosynthetic methods for $^{13}C\{^{19}F\}$ REDOR experiments. Fluorine-labeled AmB was prepared from AmB by electrophilic introduction of a fluorine atom at C14 (Scheme 2) [17]. ^{13}C-labeled AmB at the both terminal positions was obtained by feeding the microorganism with 3-^{13}C-propionic acid, by which ^{13}C was incorporated into C39, C40, and C41 (Scheme 3). Chemical synthesis of the polyene/tail portion of AmB was further carried out to obtain ^{13}C- and ^{19}F-labeled AmB at the polyene portion as depicted in Scheme 4. Solid-state NMR studies using 28-fluorinated AmB methylester (28F-AME) will be reported in due course.

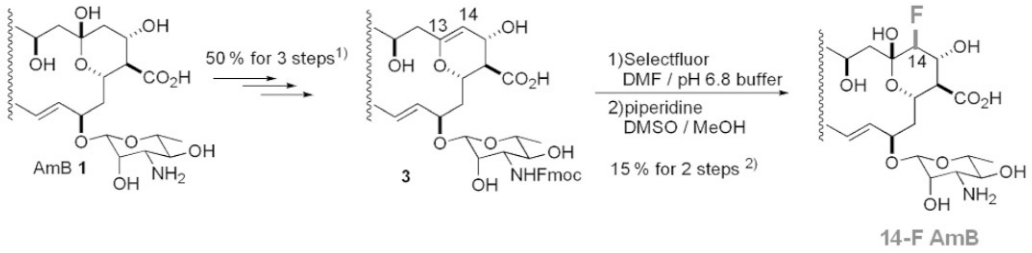

Scheme 2 Preparation of 14-fluorinated AmB (14F-AmB) [17].

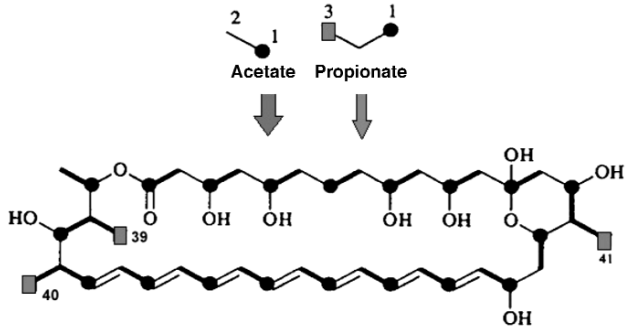

Scheme 3 Biosynthetic preparation of 39, 40, 41-tri-^{13}C-labeled AmB ($^{13}C_3$-AmB) [13].

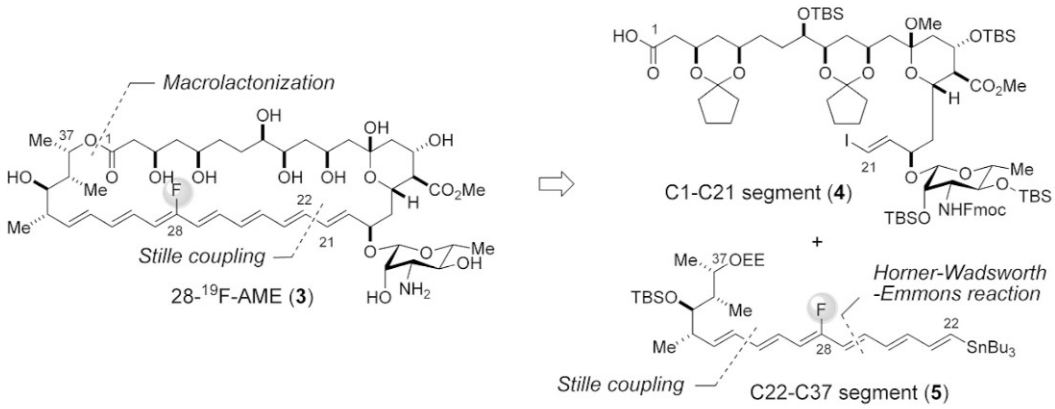

Scheme 4 Synthesis of 28F-AME. The C1–C21 segment was obtained from natural AmB while C22–C37 was synthesized chemically [18].

The 14-fluorine analog showed the biological activities comparable to those of AmB including ion channel formation and antifungal activities [17]. Unlike the AmB–sterol conjugates, covalent linkage between AmBs was particularly difficult. Thus, we attempted to estimate the ^{13}C-^{19}F distance in an intermolecular manner by ^{13}C{^{19}F} REDOR. If $^{13}C_3$-AmB and 14-F-AmB are arranged randomly in the assembly, the distance between the neighboring two molecules should be theoretically determined. As depicted in Fig. 5, the dephasing effects were shown in the both terminal parts of AmB in dimyritoylphosphatidylcholine (DMPC) membrane without sterol. The effect at C41 reveals that AmB molecules have close head-to-head interaction, where the distance between C41 and 14-F was estimated to be about 8 Å. The interactions between AmB and acyl chains of the phospholipid were also detected

in the spectra. On the other hand, the effect at C40 shows the head-to-tail orientation, which indicates that both interactions co-exist in the AmB assembly under the experimental conditions. In the presence of ergosterol, preliminary experiments revealed that similar REDOR data were observed, while the dephasing effect for C40 was somewhat attenuated. These results disclosed that, in DMPC membrane, AmB molecules interact with each other so closely as implied by the barrel-stave model. To examine the AmB interactions in other membrane systems, solid-state NMR experiments using ^{19}F-labeled AmB and ^{13}C-labeled sterol (and vice versa) are currently underway in our laboratory.

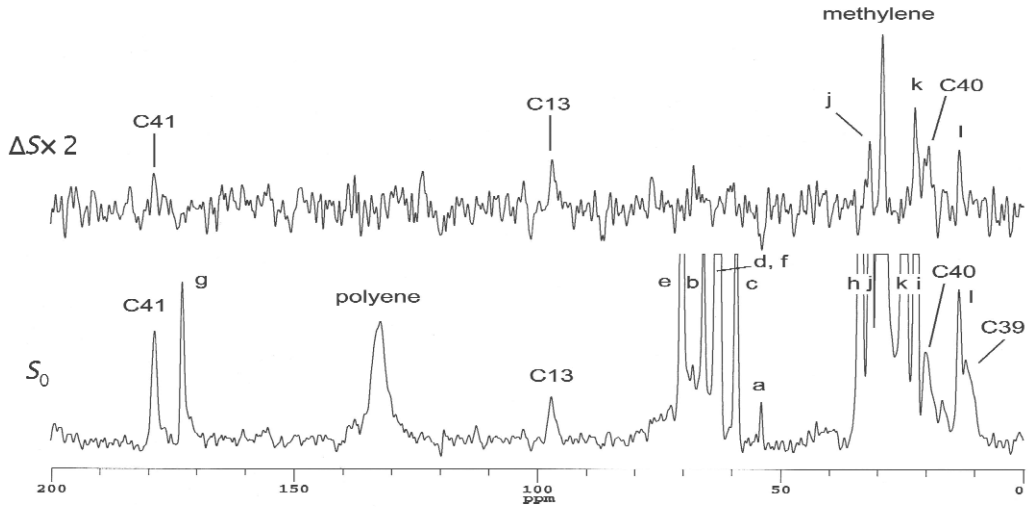

Fig. 5 ^{13}C{^{19}F} REDOR spectra of $^{13}C_3$-AmB and 14-F-AmB in DMPC membrane without sterol. Letters a–l and "methylene" denote signals due to DMPC.

ACKNOWLEDGMENTS

We are grateful to Dr. S. Matsuoka, N. Eiraku, H. Ikeuchi, Y. Matsuo, and H. Ueno for preparing labeled compounds. This study was supported by Grants-in-Aid for Scientific Research (S) (No. 18101010) and for Young Scientists (A) (No. 17681027) from MEXT, Japan. A research fellowship to S. Umegawa and N. Matsushita, from GCOE program, "Global Education and Research Center for Bio-Environmental Chemistry", is also acknowledged.

REFERENCES

1. C. Walsh. *Antibiotics: Actions, Origins, Resistance*, AMS Press, Herndon, VA (2003).
2. S. Hartsel, J. Bolard. *Trends Pharmacol. Sci.* **17**, 445 (1996).
3. A. Lemke, A. F. Kiderlen, O. Kayser. *Appl. Microbiol. Biotechnol.* **68**, 151 (2005).
4. N. Witzke, R. Bittman. *Biochemistry* **23**, 1668 (1984).
5. M. Cheron, B. Cybulska, J. Mazerski, J. Grzybowska, A. Czerwinski, E. Borowski. *Biochem. Pharmacol.* **37**, 827 (1988).
6. B. De Kruijff, R. A. Demel. *Biochim. Biophys. Acta* **339**, 57 (1974).
7. (a) T. Gullion, J. Schaefer. *Adv. Magn. Reson.* **13**, 57 (1989); (b) T. Gullion, J. Schaefer. *J. Magn. Reson.* **81**, 196 (1989); (c) A. K. Mehta, J. Schaefer. *J. Magn. Reson.* **163**, 188 (2003).
8. N. Matsumori, N. Yamaji, S. Matsuoka, T. Oishi, M. Murata. *J. Am. Chem. Soc*. **124**, 4180 (2002).
9. N. Yamaji, N. Matsumori, S. Matsuoka, T. Oishi, M. Murata. *Org. Lett.* **4**, 2087 (2002).
10. Y. Umegawa, N. Matsumori, T. Oishi, M. Murata. *Tetrahedron Lett.* **48**, 3393 (2007).

11. S. Matsuoka, M. Murata. *Biochim. Biophys. Acta* **1564**, 429 (2002).
12. N. Matsumori, N. Eiraku, S. Matsuoka, T. Oishi, M. Murata, T. Aoki, T. Ide. *Chem. Biol.* **11**, 673 (2004).
13. R. Mouri, K. Konoki, N. Matsumori, T. Oishi, M. Murata. *Biochemistry* **47**, 7807 (2008).
14. Y. Kasai, T. Oishi. Personal communication.
15. (a) G. A. Boswell Jr. U.S. Patent 4 212 815, 15 July 1980; (b) *Chem. Abstr.* **93**, 239789 (1980).
16. Y. Kasai, N. Matsumori, Y. Umegawa, S. Matsuoka, H. Ueno, H. Ikeuchi, T. Oishi, M. Murata. *Chem.—Eur. J.* **14**, 1178 (2008).
17. N. Matumori, Y. Umegawa, T. Oishi, M. Murata. *Bioorg. Med. Chem. Lett.* **15**, 3565 (2005).
18. H. Tsuchikawa, N. Matsushita, N. Matsumori, M. Murata, T. Oishi. *Tetrahedron Lett.* **47**, 6187 (2006).